



Originally published as:

Akilan, A., Abdul Azeez, K. K., Schuh, H., Yuvraaj, N. (2015): Large-Scale Present-Day Plate Boundary Deformations in the Eastern Hemisphere Determined from VLBI Data: Implications for Plate Tectonics and Indian Ocean Growth. - *Pure and Applied Geophysics*, 172, 10, pp. 2643–2655.

DOI: <http://doi.org/10.1007/s00024-014-0952-2>

1  
2  
3  
4  
5  
6  
7  
8  
9  
10  
11  
12  
13  
14  
15  
16  
17  
18  
19  
20  
21  
22  
23  
24  
25  
26  
27  
28  
29  
30  
31  
32  
33  
34  
35  
36  
37  
38  
39  
40  
41  
42  
43  
44  
45  
46  
47  
48  
49  
50  
51  
52  
53  
54  
55  
56  
57  
58  
59  
60  
61  
62  
63  
64  
65

# Large-scale present-day plate boundary deformations in the Eastern hemisphere determined from VLBI data: Implications for plate tectonics and Indian Ocean growth

A. Akilan<sup>1</sup>, K. K. Abdul Azeez<sup>1</sup>, H. Schuh<sup>2,3,4</sup> and N. Yuvraaj<sup>5</sup>

<sup>1</sup>*CSIR-National Geophysical Research Institute, Uppal Road, Hyderabad – 500007, India.*

<sup>2</sup>*GFZ, German Research Centre for Geosciences, Potsdam, Germany.*

<sup>3</sup>*Vienna University of Technology, Vienna, Austria.*

<sup>4</sup>*TU Berlin, Dept. of Geodesy and Geoinformation Science, Berlin, Germany.*

<sup>5</sup>*Prime Steels, Kolkata – 700001, India.*

## Abstract

Dynamics of the planet Earth is the manifestation of the diverse plate tectonic processes, which have been operational since the Archean period of Earth evolution and continue to deform the plate boundaries. Very Long Baseline Interferometry (VLBI) is an efficient space geodetic method that allows the precise measurement of plate motions and associated deformations. We analyze here the VLBI measurements made during a period of about three decades at five locations on the Eastern hemisphere of the globe, which are geographically distributed over five continents (plates) around the Indian Ocean. The computed baseline length rates show the deformation pattern and its rate at the boundaries between the major tectonic plates constituting the Eastern Earth hemisphere. The African

1 (Nubian) and Antarctic plates are moving apart at 13.5 mm/yr, which is mostly attributed to  
2 South West Indian Ridge spreading. Similarly, a spreading rate of 59.0 mm/yr is observed for  
3 the South East Indian Ridge that separates the Antarctic and Australian plates. Shortening at  
4 the rate of 3.9 mm/yr is estimated across the subduction boundary between Africa (Nubia)  
5 and Eurasia. Similar kind of convergence process is evident between the Australian and  
6 Sunda blocks (of the Eurasian plate). The associated deformation of -54.8 mm/yr appears to  
7 be chiefly accommodated along the Banda arc system, where the Australian plate is  
8 subducting under the Sunda block. VLBI sites within the Eurasian plate, Wettzell in Germany  
9 and Seshan on the South China block, are moving apart at a rate of 3.6 mm/yr. This relative  
10 motion between locations on the same plate is interpreted to be due to the deformation  
11 process along a large strike-slip fault, which is identified as the Western boundary of South  
12 China block. Indian Ocean expansion, at the rate of +91.5 m<sup>2</sup>/yr, is also estimated from the  
13 deformation rate estimated within the five baselines studied here. From the Hurst exponent  
14 values, which is an indicator of the future trend of a time series data, we predict the  
15 deceleration of the various tectonic processes that are operational at present.  
16  
17  
18  
19  
20  
21  
22  
23  
24  
25  
26  
27  
28  
29  
30  
31  
32  
33  
34  
35  
36

37 **Key words:** VLBI; Plate tectonics; Crustal deformation; Eastern hemisphere; Indian Ocean;  
38  
39 Hurst exponent; Strain rate.  
40  
41  
42  
43  
44  
45

46 \*corresponding author: A. Akilan, CSIR-National Geophysical Research Institute, Uppal  
47 Road, Hyderabad – 500007, India. Email: akilan@ngri.res.in; Phone: +914027012518  
48  
49  
50  
51  
52  
53  
54  
55  
56  
57  
58  
59  
60  
61  
62  
63  
64  
65

## 1. Introduction

The plate-tectonic theory envisages the movement of rigid lithosphere plates (oceanic and continental) over the ductile (convecting/weak) asthenosphere and provides an explanation to the various tectonic deformations on the Earth. Diverse kinematics of the tectonic plates include the convergence, divergence, and the strike-slip motions, which are the mechanisms responsible for the distinct tectonic deformation processes, namely the subduction, seafloor-spreading, and the occurrence of earthquakes, respectively. These tectonic processes produce small to large scale plate motions and deformations (shortening, extension, upliftment or subsidence) on the Earth surface; therefore result in surface displacements (horizontal and/or vertical) on the spherical Earth. The kinematics of the tectonic plates (plate motion velocity) and deformation of the Earth surface can be studied using terrestrial and space geodetic measurements, such as Very Long Baseline Interferometry [VLBI] (Schuh and Behrend, 2012, and references therein), Global Positioning System [GPS] (e.g. Larson and Agnew, 1991; Bouin and Vigny, 2000; Sella et al., 2002), synthetic aperture radar interferometry [InSAR] (e.g. Burgmann et al., 2000, and references therein; Garthwaite et al., 2013), and Satellite Laser Ranging [SLR] (e.g. Christodoulidis et al., 1985; Smith et al., 1990).

VLBI is a space geodetic technique that allows to determine precise coordinates on the Earth to monitor the variable Earth rotation and orientation with highest accuracy, and to derive many other parameters of the Earth system (Schuh and Behrend, 2012). VLBI is thus a highly preferred tool for geodesy (e.g. Petrov et al., 2009), geodetic astronomy (e.g. Schlüter and Behrend, 2007; Doleman et al., 2008), and geodynamics (e.g. Lyzenga et al., 1986;

1 Ward, 1990; MacMillan, and Ma, 1999; Campbell and Nothnagel, 2000; Haas et al., 2000).  
2  
3 In geodetic applications of VLBI, the difference between the arrival times of radio signals  
4  
5 emitted by deep space sources (e.g. quasars or radio galaxies) at each of the two radio  
6  
7 telescopes is measured precisely and the distance between them (i.e. the baseline length) is  
8  
9 computed. VLBI has the advantage of computing the baseline lengths that range from several  
10  
11 tens of kilometers to several thousands (~10000 km) of kilometers with sub-centimeter  
12  
13 accuracy (Herring, 1992; Schuh and Böhm, 2013), which makes it a useful and efficient tool  
14  
15 for both large (global and intercontinental, e.g. Herring et al., 1986; Ryan and Ma, 1989) and  
16  
17 local/regional scale (e.g. Clark et al., 1987; Haas et al., 2003) geodynamic studies  
18  
19 (Hinteregger et al., 1972; Whitney, 1976; Yen et al., 1991; Teke et al., 2010). VLBI is the  
20  
21 only technique today for the determination of the International Celestial Reference Frame  
22  
23 (ICRF) (Ma et al., 1990; Schuh and Böhm, 2013) and it also contributes to the realization of  
24  
25 the International Terrestrial Reference Frame (ITRF) (Böckmann et al., 2010; Altamimi et al.,  
26  
27 2011; Schuh and Böhm, 2013). Though the VLBI station distribution over the globe is  
28  
29 limited, the present array of VLBI stations is used for the precise determination of Earth  
30  
31 deformation (horizontal and vertical displacements) due to plate motions and earthquakes  
32  
33 (e.g. Petrov et al., 2009).  
34  
35  
36  
37  
38  
39  
40  
41  
42  
43

44 The Indian Ocean is the central stage for some of the prominent tectonic processes in  
45  
46 the current global geodynamics as it is the meeting point of a few major tectonic plates of the  
47  
48 Earth (Figure 1). Therefore, the kinematics and deformation of the region encompassing the  
49  
50 active plate tectonic margins would be of some interest, particularly in the global context.  
51  
52 The rate and extent of deformations associated with some of these geodynamic processes  
53  
54 were studied by several authors using geodetic measurements, chiefly employing GPS  
55  
56 geodesy (e.g. Bilham et al., 1997; Reilinger et al., 1997; Michel et al., 2001; Reilinger et al.,  
57  
58  
59  
60  
61  
62  
63  
64  
65

2006; Gahalaut et al., 2013; Yadav et al., 2013), which are mostly limited to local/regional scale. For the first time, we study here a relatively larger scale of the globe (intercontinental scale) around the Indian Ocean to understand the deformation pattern and its estimate using the more precise VLBI technique. This is achieved by calculating the intercontinental baseline length between the available VLBI sites located on the different continents surrounding the Indian Ocean. Accurate computation of baseline lengths of intercontinental scale achieved by VLBI measurements allow us to study the large scale horizontal plate motions caused by tectonic processes in this part of globe. We also speculate on the future trend of the plate tectonic motions in this region from the evaluation of the Hurst exponent.

## 2. VLBI data and analysis

In this study, VLBI measurements from five stations located on the different continents/tectonic plates in the Eastern hemisphere are used. The five measurement sites are: Wettzell (Wz) in Germany (Europe), Seshan (Sh) in China (Asia), HartRAO (Hh) in South Africa (Africa), Syowa (Sy) in Antarctica (Antarctica), and Hobart (Ho) in Australia (Australian) (Figure 1). As seen from Figure 1, the continents associated with these sites surround the Indian Ocean. Most of the VLBI stations are located reasonably away from co-seismic and post-seismic deformation zones and thus can be characterized as suitable VLBI recording points for plate motion and plate boundary deformation studies. The station Seshan, however, might have been affected by co and post-seismic deformations as indicated by the ~5 mm horizontal displacement (mainly in the east direction) during the Tohoku-Oki earthquake ( $M_w=9.0$ ) in Japan (Hooper et al., 2013). Measurement of relative continental movements and crustal deformations are possible when at least one site from each plate

1 considered for the study has taken part in a VLBI geodetic session, i.e. simultaneous VLBI  
2 recording at two different locations. If stations have a sufficient observational history in terms  
3 of number of sessions and time span, a relative linear annual drift of the plates can be  
4 estimated. This study uses the VLBI data recorded mostly from 1987 to 2013. These  
5 measurements span almost three decades and thus provide sufficient VLBI sessions to  
6 determine the rate of baseline changes (annual rate) for geodynamic and plate boundary  
7 deformation studies. The details of the VLBI sites and of the recording periods, as well as the  
8 number of sessions used for the baseline length computation are listed in Tables 1 and 2. It  
9 can be seen from Table 2 that because of operational difficulties, Syowa station located in  
10 Antarctica participated in relatively few measurements. Prior to the baseline estimation, the  
11 necessary processing of the data has been carried out. Processing contains the steps to reduce  
12 the errors including instrumental and environmental (ionosphere delay, troposphere delay,  
13 source structure delay) corrections. Details of the data reduction, corrections and further  
14 analysis to compute the baseline lengths are described in Schuh and Böhm (2013). The  
15 processing of the data is done using the software VieVS developed at Vienna University of  
16 Technology (Vienna) and the baseline lengths corresponding to each individual observing  
17 session (experiment) are computed for a particular combination of VLBI sites. The baseline  
18 length estimates for the entire period of measurements (whole data from the inception of the  
19 individual station) are further analyzed to estimate the rate of change per year, which would  
20 shed light on the ongoing tectonic movements associated with the Indian Ocean region.

21  
22  
23  
24  
25  
26  
27  
28  
29  
30  
31  
32  
33  
34  
35  
36  
37  
38  
39  
40  
41  
42  
43  
44  
45  
46  
47  
48  
49  
50  
51  
52  
53 Baseline length and its changes with time between five pairs of VLBI sites, namely  
54 HARTRAO-SYOWA, SYOWA-HOBART, WETTZELL-HARTRAO, HARTRAO-  
55 SESHAN, and WETTZELL- SESHAN, were analysed. These five baselines altogether form  
56 an envelope and almost completely encircle the Indian Ocean. The above five pairs are  
57  
58  
59  
60  
61

1 constrained by the participation of a particular site in a VLBI session (i.e. simultaneous  
2 recordings at a pair of sites). The estimated baseline lengths for each combination of sites for  
3 the available measurements are plotted against the observation time (Figure 2). A least-  
4 squares fit for the baseline length time series is carried out. The slope of the best fit line gives  
5 the rate of change of the baseline length with time. The obtained baseline length rate for the  
6 five arms considered in this study, as well as the strain rate (ratio between rate and length of  
7 baseline length), are given in Table 3. Baseline length changes between other possible  
8 combinations of stations (e.g. SESHAN-SYOWA, WETZELL-SYOWA, HARTRAO-  
9 SESHAN, etc.) were not analyzed either due to the absence or due to the lack of sufficient  
10 measurements involving those pairs.  
11  
12  
13  
14  
15  
16  
17  
18  
19  
20  
21  
22  
23  
24  
25  
26  
27  
28  
29  
30  
31  
32  
33  
34  
35  
36  
37  
38  
39  
40  
41  
42  
43  
44  
45  
46  
47  
48  
49  
50  
51  
52  
53  
54  
55  
56  
57  
58  
59  
60  
61  
62  
63  
64  
65

The law containing geological evolution can be analyzed using spectral analysis (Botezatu, 1970). The power spectra (P) of the baseline length signal observed in this study is computed using the power-law relation:

$$P(f) = P_0 f^\alpha$$

where,  $\alpha$  is the spectral index,  $P_0$  is a constant and  $f$  is the frequency (Agnew, 1992; Mao et al., 1999). The spectral index  $\alpha$  calculated for each pair is shown in Figure 2. Here, a time span of ten days corresponds to  $1.15 \times 10^{-5}$  Hz, a year corresponds to  $3.16 \times 10^{-8}$  Hz, and a time span of ten years corresponds to  $3.16 \times 10^{-9}$  Hz. There are no yearly or monthly variations seen in the power spectra. The GPS signals generally show annual and semi-annual fluctuations (Prawirodirdjo and Bock, 2004). However, such annual or monthly variations are not present with the VLBI estimations, which is an additional advantage of the VLBI data over GPS data. But, there are dips and peaks present in the power spectrum at different frequencies (or corresponding time periods), which may be due to unmodelled signals from



1 oceanic, atmospheric, or hydrological loading (e.g. Scherneck, 1991). Detailed studies on  
2 these factors are beyond the scope of this paper.  
3  
4  
5  
6  
7

8  
9 The estimated spectral index, as derived from the power spectrum analysis, is further  
10 used to estimate the Hurst exponent (Mandelbrot, 1983), which helps predicting the future  
11 trend of the plate motions in the region (e.g. Akilan, 2013). The Hurst exponent (H) is  
12 defined as:  
13  
14  
15  
16  
17

$$18 H = 1/2 (\alpha - 1)$$

19 where  $\alpha$  is the spectral index, which is obtained from the power spectrum analysis  
20 (Mandelbrot, 1983; Agnew, 1992). The Hurst exponent is a measure to classify any time  
21 series. It indicates random nature of the time series when  $H=0.5$ , while a reinforcing trend can  
22 be assumed when the value of  $H > 0.5$  (e.g. Nickolaenko et al., 2000; Qian and Rasheed,  
23 2004, 2007; Redondo, et al., 2010). Table 4 gives the estimated spectral indices and the  
24 corresponding Hurst exponents.  
25  
26  
27  
28  
29  
30  
31  
32  
33  
34  
35  
36  
37  
38  
39  
40  
41  
42

### 43 **3. Results and discussion**

44  
45  
46  
47  
48  
49 The rate of baseline length per year (baseline rate) computed for the five VLBI station  
50 pairs and the average baseline length values are shown on the simplified tectonic map of the  
51 study region (Figure 1). The baselines are approximately normal to the major plate  
52 boundaries, except the baseline between Syowa-Hobart (i.e. between Australia and Antarctic  
53 plates) that makes a sharp angle. The strain rates (ratio of changes in baseline length per year  
54  
55  
56  
57  
58  
59  
60  
61  
62  
63  
64  
65

1 to the baseline length) are also estimated between each pair of sites and are presented in  
2 Table 3 along with its baseline length rate and the average baseline lengths. Below, we  
3  
4 discuss these results and their relevance to the present day plate tectonic processes for each  
5  
6 pair of VLBI sites.  
7  
8  
9

### 10 11 12 13 3.1 HARTRAO-SYOWA 14 15 16 17 18 19

20 The average baseline length and its rate of change between the sites HartRAO in the  
21 African continent and Syowa in the Antarctic continent is estimated to be 4741786.094 m and  
22 +13.5 mm/yr, respectively. The annual rate of the baseline change of +13.5 mm/yr between  
23 these two sites indicates that these two points on two different continents move apart. The  
24 major plate tectonic process occurring in the region occupied by these two VLBI measuring  
25 points is the slow spreading Southwest Indian Ridge (SWIR). Hence, the observed increase in  
26 baseline length per year can be mostly associated with the spreading of SWIR, which is  
27 present between the Bouvet triple junction ( $54^{\circ} 17' 30''$  S,  $1^{\circ} 5' 0''$  W) in the Atlantic Ocean  
28 and the Rodrigues triple junction ( $25^{\circ} 30'$  S,  $70^{\circ} 0'$  E) in the Indian Ocean. Sempere and  
29 Klein (1995) showed a slow spreading between 13 and 18 mm/yr for the SWIR, which is quite  
30 consistent with our result. DeMets et al. (1988) also previously obtained similar spreading  
31 rates (14-18 mm/yr) across the SWIR. DeMets et al. (1994, 2010) also computed spreading  
32 rates within this range. Therefore it is reasonable to conclude that the deformations occurring  
33 between the African plate and the Antarctic plate are solely due to the divergent tectonics  
34 along the SWIR. The Marion hotspot spotted near to the SWIR may possibly influence the  
35 SWIR spreading rate and the pattern due to the hotspot interaction with the ridge (Tao et al.,  
36 2011).  
37  
38  
39  
40  
41  
42  
43  
44  
45  
46  
47  
48  
49  
50  
51  
52  
53  
54  
55  
56  
57  
58  
59  
60  
61  
62  
63  
64  
65

### 3.2 SYOWA-HOBART

The VLBI stations, Syowa located on the Antarctic plate and Hobart located on the Australian plate, give an average baseline length of 6035892.681 m and a higher baseline rate of +59.0 mm/year. The higher elongation rate (baseline length change per year) estimated for this pair suggests much faster divergence between the two plates (i.e. Australia and Antarctica) involved in the VLBI measurement. The prominent tectonic element separating these two tectonic plates is the (NW-SE trending) Southeast Indian Ridge (SEIR) that extends from Rodrigues triple junction ( $25^{\circ} 30'S$ ,  $70^{\circ} 0'E$ ) to Macquarie triple junction ( $61^{\circ} 30'S$ ,  $161^{\circ} 0'E$ ). Previously determined spreading rate values over the SEIR range from 58 to 76 mm/yr (Sempere and Klein, 1995) and our VLBI based baseline length change per year across this feature also falls within this range. DeMets et al. (1988) also reported ridge normal spreading rate of  $\sim 68$  mm/yr, which later was agreed by the NUVEL-1 plate motion model (DeMets et al., 1990). The recent MORVEL (DeMets et al., 2010) plate motion model estimated values between 60-70 mm/yr spreading rate between Australia and Antarctic plates. Small (1995) showed the influence of hotspots on ridge spreading through ridge-hotspot interactions and suggested the role of Kerguelen hotspot in promoting the spreading at SEIR. Since there is no significant crustal deformation within the Australian plate (Larson et al., 1997) and the VLBI horizontal deformation rate match with the spreading rate estimated at SEIR, we can confidently argue that the +59 mm/yr baseline rate represents mostly the divergence rate across the SWIR. The findings from the present VLBI study corroborate with Conder and Forsyth (2001) who showed a region of extension in the SEIR as a consequence of which the distance between Antarctica and Australia is increasing.

### 3.3 WETTZELL-HARTRAO

The VLBI measurements made by the participation of Wettzell (Germany, European plate) and HartRAO (African plate) give an average value of 7832322.470 m and a rate of -3.9 mm/yr for the baseline length between them. The boundary zone between the African and Eurasian plates encompass the region of the Mediterranean Sea and Middle East and represent the collision zone between Africa and Eurasia, which lead to the progressive closure of Tethys Ocean since the Cretaceous and the deformation process still continues at present (e.g. Lustrino et al., 2011 and references therein). The computed rate of baseline length (-3.9 mm/yr) between Wettzell and HartRAO must be representing the overall deformation occurring between Eurasia and Africa, and well supports the convergent (subduction) geodynamics between the above two plates. The GPS data from the Western part of the Africa-Eurasia collision zone (plate boundary) suggests that this segment accommodates about 2-4 mm/yr of SE-NW convergence (Serpelloni et al., 2007). This estimate very well matches with our VLBI estimated convergence rate. Kreemer et al. (2003) also predicted a convergence rate of ~4 mm/yr for the subduction between African (Nubian) and Eurasian plates. The NUVEL-1 plate motion model (DeMets et al., 1990) predicted comparable values (4-6 mm/yr) for the Africa-Eurasia convergence. The recent NUVEL-1A (DeMets et al., 1994) and MORVEL (DeMets et al., 2010) plate motion models also calculated similar deformation rate of  $4 \pm 0.2$  mm/yr between Africa and Eurasia. The deformation within the African plate is found to be negligible for a N-S section of Africa (e.g. Royer et al., 1997) and the Eurasian plate appears to be a rigid one (Prawirodirdjo and Bock, 2004). Thus, the value of -3.9 mm/yr possibly indicates the convergence rate between the African and Eurasian lithospheres, which is totally accommodated within the collision plate boundary between the two plates.

### 3.4 WETTZELL-SESHAN

1  
2  
3  
4  
5  
6 VLBI estimates show that the baseline length between the stations Wettzell and  
7  
8 Seshan is lengthening at the rate of 3.6 mm/yr. Both sites (Wettzell and Seshan) are part of  
9  
10 the Eurasian plate, which appears to be rigid at its interior (Prawirodirdjo and Bock, 2004).  
11  
12 Station Wettzell is located in central Europe, where GPS data showed negligible intraplate  
13  
14 velocity (e.g. Grenerczy et al., 2000). On the other hand, the site Seshan located on the South  
15  
16 China block shows an East to Southeast movement at present as implied from GPS velocity  
17  
18 vectors (Vergnolle et al., 2007). The seismological and geologic data together with analysis  
19  
20 of Landsat imagery suggested no deformation within the South China block (cf. Vergnolle et  
21  
22 al., 2007). The Western boundary of this block is marked with the large strike-slip fault zone  
23  
24 (Longmen fault zone) and represents a localized deformation zone. The South China block in  
25  
26 the Southeastern margin of Eurasia is thus seen to be a continuously deforming zone attached  
27  
28 to the Eurasian plate (e.g. Kreemer et al., 2000). GPS results suggest that the South China  
29  
30 block (as well as the North China block) is decoupled from Eurasia and moves Eastward with  
31  
32 a velocity of 4-13 mm/yr (Heki et al., 1999; Shen et al., 2000; Chen et al., 2000). This  
33  
34 deforming zone, representing the Western boundary of the South China block, can be  
35  
36 therefore thought as the most responsible region where the observed divergence between the  
37  
38 two VLBI sites on the Eurasian plate is accommodated. The divergence in this part might  
39  
40 have been the result of the Eastward pulling of South China block due to tensional and  
41  
42 oceanward stresses generated by the active margins of Eastern and Southeastern Asia or other  
43  
44 subduction processes (Vergnolle et al., 2007). Previous VLBI study by Molnar and Gipson  
45  
46 (1996) have showed similar east-southeast relative movement of south China block at ~8  
47  
48 mm/yr with respect to Eurasian plate. Calais et al. (2006) showed horizontal motion rates  
49  
50  
51  
52  
53  
54  
55  
56  
57  
58  
59  
60  
61  
62  
63  
64  
65

1 varying from 0 to about 9 mm/yr from North to South across North and South China, which  
2 qualitatively agrees with the VLBI observation.  
3  
4  
5  
6  
7

### 8 9 3.5 SESHAN-HOBART

10  
11  
12  
13  
14  
15 The baseline length between Hobart and Seshan stations shows a convergence at the  
16 rate of 54.8 mm/yr. Seshan and Hobart belongs to two separate tectonic plates, i.e. Eurasia  
17 and Australia plate, respectively. The South China microplate carrying the Seshan site, as  
18 well as the Australain plate holding Hobart, do not show any significant internal deformation  
19 (Larson et al. 1997; Tregoning, 2002; Bock et al., 2003; Vergnolle et al., 2007). Three major  
20 tectonic plates, namely the Sunda block, the Philippine, and the Pacific, collectively separate  
21 the South China block from the Australian plate (e.g. Michel et al., 2001; Simons et al.,  
22 2007). This region that abuts with the Australian plate is the locus of complex active  
23 subduction zone systems involving the adjacent Philippine, the Australian, and the Indian  
24 plates. The observed convergence in our VLBI measurements can be attributed to the active  
25 deformation resulting from the ongoing Northward subduction of the Australian plate with  
26 the Sunda and the Pacific plates. It is, however, difficult from our study to point out which  
27 among these subduction/collision systems dominate the observed convergence rate, due to the  
28 complex tectonics arising from the collision/subduction that occurs between the Australian  
29 lithosphere and the complex block assemblage in the area of triple junction between the  
30 Sunda block, the Pacific plate, and the Australian plate. Nevertheless, the present study  
31 confirms the overall active subduction/collision processes in the region. GPS studies gave a  
32 convergence rate of 66-72 mm/yr between the Sunda block and the Australian plate (Michel  
33 et al., 2001). Bock et al. (2003) estimated a shortening rate of 50 mm/yr occurring between  
34  
35  
36  
37  
38  
39  
40  
41  
42  
43  
44  
45  
46  
47  
48  
49  
50  
51  
52  
53  
54  
55  
56  
57  
58  
59  
60  
61  
62  
63  
64  
65

1 the Australia and the Sunda block at the Banda Arc. Simons et al. (2007) estimated  
2 shortening rate of ~70 mm/yr, which showed compatibility with the MORVEL plate motion  
3 models reported varying convergence rate of 60 – 73 mm/yr along the Australia-Sunda block  
4 boundary (DeMets, 2010).  
5  
6  
7  
8  
9

10  
11  
12  
13  
14 Plate boundaries are important as these are the locations where the continental crust is  
15 either generated or destroyed. The VLBI computed baseline length and its rate of change  
16 between sites located on the major tectonic plates thus provide evidence for the plate tectonic  
17 processes and associated tectonic deformations occurring along the plate boundaries between  
18 these major lithospheric plates. It is quite evident that the African, the Eurasian, and the  
19 Australian plates are drifting away from the Antarctic plate, as shown by the positive baseline  
20 rates estimated between the Antarctic VLBI station (Syowa) and the sites in the other three  
21 plates. It is reasonable to infer from the ongoing shortening between Africa and Eurasia, as  
22 well as between SE Asia and Australia, that the continents Africa and Europe are nearing  
23 each other, and similarly Asia and Australia are slowly coming closer.  
24  
25  
26  
27  
28  
29  
30  
31  
32  
33  
34  
35  
36  
37  
38  
39  
40  
41

42 The strain rate ( $\Delta/l$ ) computed for the baselines gives positive strain values between  
43 HartRAO and Syowa ( $2.847 \times 10^{-9} \text{ y}^{-1}$ ), and Syowa and Hobart ( $9.775 \times 10^{-9} \text{ y}^{-1}$ ). Such  
44 extensional strain values along the plate boundaries represented by these VLBI sites are  
45 indicative of low seismic activity. This inference agrees with the relatively low seismicity  
46 reported (e.g. see Figure 5 in Sella et al., 2002) along the SWIR and SEIR ridges separating  
47 the tectonic plates representing the above sites. Strain rates of  $-6.880 \times 10^{-9} \text{ y}^{-1}$  and  $-4.979 \times$   
48  $10^{-10} \text{ y}^{-1}$  are computed for other two major segments, Hobart-Seshan and HartRAO-Wettzell,  
49 respectively. This accumulation of strain along these tectonic boundaries characterizes them  
50  
51  
52  
53  
54  
55  
56  
57  
58  
59  
60  
61  
62  
63  
64  
65

1 as prone zones for vigorous seismic activity. Our results are consistent with Kreemar et al.  
2 (2003) results, which showed high compressive strain rates along these plate boundaries. The  
3 generation of high magnitude earthquakes with relatively high frequency along these plate  
4 boundary subduction zones validates the VLBI observations. The presence of many  
5 earthquakes in the Northern part of the Indian Ocean (North of Australia), as compared to the  
6 few seismic events reported from its Southern part (South of Australia) (e.g. Bergman and  
7 Solomon, 1980) supports our present observations of higher strain concentration in the North-  
8 East Indian Ocean region between the Sunda block and the Australian plate. Bock et al. (2003)  
9 showed strain rates below  $5 \times 10^{-8} \text{ y}^{-1}$  for the larger part of the region between the Sunda  
10 block and Australia. Large earthquakes are frequently reported from the subduction boundary  
11 between the Indian plate and the Sunda block (Eurasian plate). The Indian Ocean earthquakes  
12 from the Sumatra region are some recent examples (e.g. Yadav et al., 2013; Catherine, et al.,  
13 2014). Vigorous seismicity is also evident from the subduction zone boundary between  
14 Africa and Eurasia (e.g. Bucci et al., 2010, and references therein) for which VLBI estimated  
15 a significantly high strain rate.  
16  
17  
18  
19  
20  
21  
22  
23  
24  
25  
26  
27  
28  
29  
30  
31  
32  
33  
34  
35  
36  
37  
38  
39  
40

### 41 *3.6 Implications for Indian Ocean growth*

42  
43  
44  
45

46 The five baselines considered in our study cut across the major deformation zones  
47 between the five major tectonic plates and form five arms that encircle the Indian Ocean  
48 (Figure 1). Deformations, either in the form of convergence or divergence, occurring across  
49 the tectonic boundaries are derived from the present VLBI data, as well as from previous  
50 geological and geophysical studies. VLBI results have shown varying rates for the expansion  
51 or contraction occurring across these boundaries and allow us to calculate the rate of change  
52  
53  
54  
55  
56  
57  
58  
59  
60  
61  
62  
63  
64  
65



in perimeter and area bounded by these arms. The change in perimeter (obtained from the addition of individual baseline rates) is +35.7 mm/year, which means that the boundary of the Indian Ocean is increasing at the rate of ~35.7 mm per year. Similarly, we computed the area bounded by these five baseline arms using the formula:

$$Area = \sqrt{\frac{(S-a)(S-b)(S-c)(S-d)(S-e)}{2}}$$

here,  $S = \frac{a+b+c+d+e}{2}$ ; and a, b, c, d, and e represent the five sides. The area computed for the region encompassed by these five baseline lengths thus shows an increase at the rate of 91.5 m<sup>2</sup>y<sup>-1</sup>. This implies that the Indian Ocean is expanding, however small it may be, regardless of the complex combination of divergence and convergence tectonic processes that operate within its vicinity. Our VLBI results showed the presence of both divergence and convergence process at major tectonic boundaries involving the Indian Ocean. The calculated annual increase in Indian Ocean area would thus mean that extensional deformation (divergence rate) dominates over the contractional deformation (convergence rate) and the whole processes put together gives the observed yearly growth of the Indian Ocean.

### 3.7 Speculation on the future plate tectonic processes

The Hurst exponent computed from the times series data of baseline values are presented in Table 4. It is obtained from the decay of power spectra of the observed baseline length time series for the particular pair of stations. The value of this exponent tells us the relative tendency of a time series to either regress to a long term mean value or 'cluster' in a direction. By definition, a Hurst exponent value of 0.5 (or close to 0.5) indicates a random walk motion (a Brownian time series), which does not provide any correlation between the

1 future elements. But a value of the Hurst exponent less than 0.5 indicates an “anti-persistent”  
2 behavior (trend reversal) of the time series, which would mean that an increasing trend will  
3  
4 be followed by a decreasing trend and vice-versa. A Hurst exponent value above 0.5 indicates  
5  
6 a “persistent” nature of the time series under investigation (Qian and Rasheed, 2007).  
7  
8  
9

10  
11 Here, Hurst exponent values in the range of 0.3575-0.3585 were obtained for the baseline  
12  
13 pairs considered in our study. These values are certainly below 0.5 and thus indicate an “anti-  
14  
15 persistent” behavior of the baseline time series over a out three decades of data analyzed in  
16  
17 this study. The obtained low values of the Hurst exponent are indicative of the slowdown of  
18  
19 ongoing plate tectonic processes and possibly point to the deceleration of the plate  
20  
21 movements in the future. Such an observation was also made by Edmundo et al. (1999) and  
22  
23 Sella et al. (2002). Their study argued a possible long-term deceleration associated with the  
24  
25 continental collision from the relatively slow movement of the plate pairs with respect to the  
26  
27 NUVEL-1A model. Unfortunately, the present study is unable to give any time estimate for  
28  
29 the possible deceleration of the plate movements.  
30  
31  
32  
33  
34  
35  
36  
37  
38  
39  
40

#### 41 **4. Summary and conclusions**

42  
43  
44  
45  
46

47 In this study, the VLBI space geodetic technique is used to measure the large-scale  
48  
49 deformation across the plate boundaries formed by the major tectonic plates of the Eastern  
50  
51 hemisphere. VLBI measurements were available for almost three decades from five sites  
52  
53 located over different tectonic plates, i.e. Wettzell in Germany (Eurasian plate), Seshan in  
54  
55 China (South China block of Eurasian plate), HartRAO in South Africa (African plate),  
56  
57 Syowa in Antarctica (Antarctic plate), and Hobart in Australia (Australian plate). Baseline  
58  
59  
60  
61  
62  
63  
64  
65

1 lengths corresponding to all the individual measurements, were estimated for five VLBI  
2 pairs: HARTRAO-SYOWA, SYOWA-HOBART, WETTZELL-HARTRAO, HOBART-  
3  
4 SESHAN, and WETTZELL-SESHAN, which form five arms around the Indian Ocean  
5  
6 region. The time series of the baseline lengths are analyzed statistically to determine its  
7  
8 annual rate of change occurring along each arm.  
9  
10

11  
12  
13  
14  
15  
16 Our study gives spreading rates of 13.5 mm/yr and 59.0 mm/yr for the South West  
17  
18 Indian Ridge (SWIR) and South East Indian Ridge (SEIR), respectively. SWIR separates the  
19  
20 African (Nubian) plate from the Antarctic plate and its spreading appears to be responsible  
21  
22 for the movement between Africa and Antarctic plates. Similarly, SEIR acts as the boundary  
23  
24 line between Australian and Antarctic plates and contributes the observed divergence  
25  
26 between these two plates. A shortening/convergence of 3.9 mm/yr is observed for the  
27  
28 subduction zone boundary between African (Nubian) and Eurasian plates. Such a  
29  
30 convergence is clearly evident between the Australian and Sunda block (of the Eurasian  
31  
32 plate), but the deformation is occurring at a much faster rate of -54.8 mm/yr. It appears that a  
33  
34 major part of this deformation is accommodated along the Banda arc system, where the  
35  
36 Australian plate subducts under the Sunda block. The South China block, a microplate within  
37  
38 the Eurasian plate was found to be moving away from the rest of the Eurasian block with a  
39  
40 speed of 3.6 mm/yr. We also estimate an annual increase of 91.5 m<sup>2</sup> in the area of Indian  
41  
42 Ocean from the deformation rates observed along the five VLBI baseline arms surrounding  
43  
44 the Indian Ocean. Finally, the estimated Hurst exponent values (~0.35), which can be  
45  
46 considered as an indicator for future behavior of times series, show the deceleration of the  
47  
48 various tectonic processes in the near future. We could here discuss only the important  
49  
50 broader scale deformations of plate boundaries associated with the Indian Ocean. There are,  
51  
52 however, many important and complex deformation processes happening between the  
53  
54  
55  
56  
57  
58  
59  
60  
61  
62

1 Northern and Eastern margin of the Indian plate. Thorough understanding of these processes  
2 and deformations would be possible with a more improved VLBI network including stations  
3  
4 on the Indian plate.  
5  
6  
7  
8  
9  
10

## 11 **Acknowledgements**

12  
13  
14  
15  
16  
17  
18 First author, Akilan, sincerely acknowledges Prof. Johannes Böhm for the financial  
19 assistance, as well as other logistical and scientific support, to make a successful visit to the  
20  
21 Department of Geodesy and Geoinformatics, Vienna University of Technology. The authors  
22  
23 gratefully acknowledge the IVS and all its contributing components for supporting this  
24  
25 research work with the necessary resources. Thanks also go to Dr. Y. J. Bhaskar Rao,  
26  
27 Director, CSIR-NGRI for the kind permission to publish this work. Dr. Malaimani and Dr. V.  
28  
29 Gahalaut are acknowledged for the support and facilities provided at NGRI. Figure 1  
30  
31 presented in this paper is generated using GMT software (Paul and Wessel, 1998). We  
32  
33 acknowledge the critical comments from two anonymous reviewers that helped to improve  
34  
35 the manuscript. The work has been carried out under the ILP-0301-28(VKG).  
36  
37  
38  
39  
40  
41  
42  
43  
44  
45  
46

## 47 **References**

48  
49  
50  
51  
52  
53 Agnew, D. C. (1992), The time domain behaviour of power law noise, Geophysical Research  
54  
55 Letters, 19 (4), 333-336.  
56  
57  
58  
59  
60  
61  
62  
63  
64  
65

- 1 Akilan, A., Balaji, S., Srinivas, Y., and Yuvaraj, N. (2013), Plate motion predictability using  
2 Hurst exponent applied to the Maitri-Antarctica GPS network, *Journal of Geological*  
3 *Society of India*, 82, 613-620.  
4  
5  
6  
7  
8 Altamimi, Z., Collilieux, X., and Métivier, L. (2011), ITRF2008: an improved solution of the  
9 international terrestrial reference frame, *Journal of Geodesy*, 85(8), 457-473.  
10  
11  
12  
13 Bergman, E. A., and Solomon S. C. (1980), Oceanic Intra plate earthquakes: Implications for  
14 local and regional intraplate stress, *Journal of Geophysical Research*, 85 (B10), 5389-  
15 5410.  
16  
17  
18  
19  
20  
21  
22 Bilham, R., Larson, K., Freymuller, J., and Project Idylhim members (1997), GPS  
23 measurements of present-day convergence across Nepal Himalaya, *Nature*, 386, 61-64.  
24  
25  
26  
27  
28 Bock, Y., Prawirodirdjo, L., Genrich, J. F., Stevens, C. W., McCaffrey, R., Subarya, C.,  
29 Puntodewo, S. S. O., and Calais, E. (2003), Crustal motion in Indonesia from Global  
30 Positioning System measurements, *Journal of Geophysical Research*, 108 (B8), 2367,  
31 doi: 10.1029/2001JB000324.  
32  
33  
34  
35  
36  
37  
38 Böckmann, S., Artz, T., and Nothnagel, A. (2010), VLBI terrestrial reference frame  
39 contributions to ITRF2008, *Journal of Geodesy*, 84 (3), 201-219.  
40  
41  
42  
43  
44 Botezatu, R. (1970), On the possibilities of using the power spectrum in some geological and  
45 geophysical application, *Mathematical Geology*, 2(3), 303-305.  
46  
47  
48  
49  
50 Bouin, M. N., and Vigny, C. (2000), New constraints on Antarctic plate motion and  
51 deformation from GPS data, *Journal of Geophysical Research*, 105, 28279-28293.  
52  
53  
54  
55  
56 Bucci, D. D., Burrato, P., Vannoli, P., and Valensise, G. (2010), Tectonic evidence for the  
57 ongoing Africa-Eurasia convergence in central Mediterranean foreland areas: A  
58  
59  
60  
61

1 journey among long-lived shear zones, large earthquakes, and elusive fault motions,  
2 Journal of Geophysical Research, 115, B12404, doi: 10.1029/2009JB006480.  
3

4  
5 Burgmann, R., Rosen, P. A., and Feilding, E. J. (2000), Synthetic aperture radar  
6 intererometry to measure Earth's surface topography and its deformation, Annual  
7 Review Earth Planet Science, 28, 169-209.  
8  
9

10  
11 Calais, E., Dong, L., Wang, M., Shen, Z., and Vergnolle, M. (2006) Continental deformation  
12 in Asia from a combined GPS solution, Geophysical Research Letters, 33, L24319,  
13 doi: 10.1029/2006/GL028433.  
14  
15

16  
17 Campbell, J., and Nothnagel, A. (2000), European VLBI for crustal dynamics, Journal of  
18 Geodynamcis, 30, 321-326.  
19  
20

21  
22 Catherine, J. K., Gahalaut, V. K., Srinivas, N., Kumar, S., and Nagarajan, B. (2014),  
23 Evidence of strain accumulation in the Andaman region for the giant 2004 Sumatra  
24 Andaman earthquake, Bulletin of Seismological Society of America, 104, doi:  
25 10.1785/01120130141.  
26  
27

28  
29 Chen, Z., Burchfiel, B. C., Liu, Y., King, R. W., Royden, L. H., Tang, W., Wang, E., Zhao,  
30 J., and Zhang, X. (2000), Global positioning system measurements from eastern Tibet  
31 and their implications for India/Eurasia intercontinental deformation, Journal of  
32 Geophysical Research, 105, 16215-16227.  
33  
34  
35  
36  
37

38  
39 Christodoulidis, D. C., Smith, D. E., Kolenkiewicz, R., Dunn, P. J., Klosko, S. M., Torrence,  
40 M. H., Fricke, S., and Blackwell, S. (1985), Observing tectonic plate motions and  
41 deformations from satellite laser ranging, Journal of Geophysical Research, 90, 9249-  
42 9264.  
43  
44  
45  
46  
47  
48  
49  
50  
51  
52  
53  
54  
55  
56  
57  
58  
59  
60  
61  
62  
63  
64  
65

- 1 Clark, T. A., Gorden, D., Himwich, W. E., Ma, C., Mallama, A., and Ryan, J. M. (1987),  
2 Determination of the relative site motions in the western United States using MarkIII  
3 very long baseline interferometry, *Journal of Geophysical Research*, 92, 12741-12750.  
4  
5  
6  
7  
8 Conder, J. A., and Forsyth, D. W. (2001), Seafloor spreading on the southeast Indian ridge  
9 over the one million years: a test of the Capricorn plate hypothesis, *Earth and Planetary  
10 Science letters*, 188, 91-105.  
11  
12  
13  
14  
15  
16 DeMets, C., Gordon, R. G., and Argus, D. F. (1988), Intraplate deformation and closure of  
17 the Australia-Antarctica-Africa Plate circuit. *Journal of Geophysical Research*, 93,  
18 11877-11897.  
19  
20  
21  
22  
23  
24 DeMets, C., Gordon, R. G., Argus, D. F., and Stein, S. (1990), Current plate motions.  
25 *Geophysical Journal International*, 101, 425-478.  
26  
27  
28  
29  
30 DeMets, C., Gordon, R. G., Argus, D. F., and Stein, S. (1994), Effect of recent revisions to  
31 the geomagnetic reversal time scale on estimates of current plate motions. *Geophysical  
32 Research Letters*, 21, 2191-2194.  
33  
34  
35  
36  
37  
38 DeMets, C., Gordon, R. G., and Argus, D. F. (2010), Geologically current plate motions.  
39 *Geophysical Journal International*, 181, 1-80.  
40  
41  
42  
43  
44 Doeleman, S. S., Weintroub, J., Rogers, A. E. E., Plambeck, R., Freund, R., Tilanus, R. P. J.,  
45 Friberg, P., Ziurys, L. M., Moran, J. M., Corey, B., Young, K. H., Smythe, D. L.,  
46 Titus, M., Marrone, D. P., Cappallo, R. J., Bock, D. C.-J., Bower, G. C., Chamberlin,  
47 R., Davis, G. R., Krichbaum, T. P., Lamb, J., Maness, H., Niell, A. E., Roy, A.,  
48 Strittmatter, P., Werthimer, D., Whitney, A. R., and Woody, D. (2008), Event-  
49 horizon-scale structure in the super massive black hole candidate at the Galactic centre,  
50 *Nature*, 455, 78-80.  
51  
52  
53  
54  
55  
56  
57  
58  
59  
60  
61  
62  
63  
64  
65

1 Edmundo O. N., Timothy H. D., Stein, S., and Harrison, C. G. A. (1999), Decelerating Nazca-South  
2 America and Nazca-Pacific Plate Motions, *Geophysical Research Letters*, 26, 3405-3408.  
3

4  
5 Gahalaut, V. K., Kundu, B., Laishram, S. S., Catherine, J., Kumar, A., Singh, M. D., Tiwari,  
6  
7 R. P., Chadha, R. K., Samanta, S. K., Ambikapathy, A., Mahesh, P., Bansal, A., and  
8  
9 Narsaiah, M. (2013), Aseismic plate boundary in the Indo-Burmese wedge, northwest  
10  
11 Sunda Arc, *Geology*, 41, 235-238.  
12  
13  
14

15  
16 Garthwaite, M. C., Wang, H., and Wright, T. J. (2013), Broadscale interseismic deformation  
17  
18 and fault slip rates in the central Tibetan Plateau observed using InSAR, *Journal of*  
19  
20 *Geophysical Research*, 118, 5071-5083.  
21  
22  
23

24 Grenerczy, G., Kenyeres, A., and Fejes, I. (2000), Present crustal movement and strain  
25  
26 distribution in Central Europe inferred from GPS measurements, *Journal of*  
27  
28 *Geophysical Research*, 105, 21835-21846.  
29  
30  
31

32 Haas, R., Gueguen, E., Scherneck, H. G., Nothnagel, A., and Campell. J. (2000), Crustal  
33  
34 motion results derived from observations in the European geodetic VLBI network,  
35  
36 *Earth Planet Space*, 52, 759-764.  
37  
38  
39

40 Haas, R., Nothnagel, A., Campell. J., and Gueguen, E. (2003), Recent crustal movements  
41  
42 observed with the European VLBI network: geodetic analysis and results, *Journal of*  
43  
44 *Geodynamics*, 35, 391-414.  
45  
46  
47

48 Heki, K., Miyazaki, S., Takahashi, H., Kasahara, M., Kimata, F., Miura, S., Vasilenko, N. F.,  
49  
50 Ivashchenko, A., and An, K. D. (1999), The Amurian plate motion and current plate  
51  
52 kinematics in eastern Asia, *Journal of Geophysical Research*, 104, 29147-29155.  
53  
54  
55

56  
57 Herring, T. A. (1992), Sub millimeter Horizontal Position Determination Using Very Long  
58  
59 Baseline Interferometry, *Journal of Geophysical Research*, 97, 1981-1990.  
60  
61



1 Herring, T. A., Shapiro, I. I., Clark, T. A., Ma, C., Ryan, J. W., Schuple, B. R., Knight, C. A.,  
2 Lundqvist, G., Shaffe, D. B., Vandenberg, N. R., Corey, B. E., Hinteregge, H. F., Roger,  
3 R. A., Webbe, J. C., Whitney, A. R., Elgered, G., Ronnang, B. O., and Davis, J. L.  
4 (1986), Geodesy by radio interferometry: Evidence from contemporary plate motion,  
5 Journal of Geophysical Research, 91, 8341-8347.  
6

7 Hinteregger, H. F., Shapiro, I. I., Robertson, D. S., Knight, C. A., Ergas, R. A., Whitney, A.  
8 R., Rogers, A. E. E., Moran, J. M., Clark, T. A., and Burke, B. F. (1972), Precision  
9 Geodesy via Radio Interferometry, Science, 178, 396-398.  
10

11 Hooper, A., Pietrzak, J., Simons, W., Cui, H., Riva, R., Naeije, M., Terwisscha van  
12 Scheltinga, A., Scharma E., Stelling, G., and Socquet A, (2013), Importance of  
13 Horizontal Seafloor Motion on Tsunami Height for the 2011 Mw=9.0 Tohoku-Oki  
14 earthquake, Earth and Planetary Science Letters, 361, 469-479, doi:  
15 10.1016/j.epsl.2012.11.013.  
16

17 Kreemer, C., Holt, W. E., Goes, S., and Govers, R. (2000), Active deformation in eastern  
18 Indonesia and the Philippines from GPS and seismicity data, Journal of Geophysical  
19 Research, 105, 663-680.  
20

21 Kreemer, C., Holt, W. E., and Haines, J. (2003), An integrated global model of present day  
22 plate motion and plate boundary deformation, Geophysical Journal International, 154,  
23 8-34.  
24

25 Larson, K. M., and Agnew, D. C., (1991). Application of the Global Positioning System to  
26 Crustal deformation measurement 1. Precision and accuracy, Journal of Geophysical  
27 Research, 96, 16547-16565.  
28

- 1  
2  
3  
4  
5  
6  
7  
8  
9  
10  
11  
12  
13  
14  
15  
16  
17  
18  
19  
20  
21  
22  
23  
24  
25  
26  
27  
28  
29  
30  
31  
32  
33  
34  
35  
36  
37  
38  
39  
40  
41  
42  
43  
44  
45  
46  
47  
48  
49  
50  
51  
52  
53  
54  
55  
56  
57  
58  
59  
60  
61  
62  
63  
64  
65
- Larson, K. M, Fremueller, J. T., and Philipsen, S. (1997), Global plate velocities from Global Positioning System, *Journal of Geophysical Research*, 102, 9961-9981.
- Lustrino, M., Duggen, S., and Rosenberg, C. L. (2011), The central-western Mediterranean: Anomalous igneous activity in an anomalous collisional tectonic setting, *Earth-Science Reviews*, 104, 1-40.
- Lyzenga, G. A., Wallace, K. S., Fanselow, J. L., Raefsky, A., and Groth, P. M. (1986), Tectonic motions in California inferred from Very Long Baseline Interferometry observations, 1980-1984, *Journal of Geophysical Research*, 91, 9473-9487.
- Ma, C., Sauber, M., Bell, L.J., Clark, T.A, Gorden, D., Himwich, W.E., and Ryan, J.W. (1990), Measurement of horizontal motions in Alaska using very long baseline interferometry, *Journal Geophysical Research*, 95, 21,991-22,011.
- MacMillan, D. S., and Ma, C. (1999), VLBI measurements of Caribbean and South American motion, *Geophysical Research Letters*, 26, 919-922.
- Mandelbrot, B. (1983), *The Fractal Geometry of Nature*, W. H. Freeman and company, San Francisco.
- Mao, A. (1999), Noise in GPS coordinates time series, *Journal of Geophysical Research*, 104, 2797-2816.
- Michel, G. W, Yu, Y. Q., Zhu, S. Y., Reigber, C., Becker, M., Reinhart, E., Simons, W., Ambrosius, B., Morgan, P., and Matheussen, S. (2001), Crustal motion and block behavior in SE-Asia from GPS measurements, *Earth and Planetary Sciences*, 187, 239-244.

- 1  
2  
3  
4  
5  
6  
7  
8  
9  
10  
11  
12  
13  
14  
15  
16  
17  
18  
19  
20  
21  
22  
23  
24  
25  
26  
27  
28  
29  
30  
31  
32  
33  
34  
35  
36  
37  
38  
39  
40  
41  
42  
43  
44  
45  
46  
47  
48  
49  
50  
51  
52  
53  
54  
55  
56  
57  
58  
59  
60  
61  
62  
63  
64  
65
- Molnar, P., and Gipson, J. M. (1996), A bound on the rheology of continental lithosphere using very long baseline interferometry: The velocity of south China with respect to Eurasia, *Journal of Geophysical Research*, 101, 545-553.
- Nickolaenko, A. P., Price, C., and Iudin, D. D. (2000), Hurst exponent derived for natural terrestrial radio noise in Schumann resonance band, *Geophysical Research Letters*, 27, 3185-3188.
- Petrov, L., Gordon, D., Gipson, J., MacMillan, D., Ma, C., Fomalont, E., Walker, R. C., and Carabajal, C. (2009), Precise Geodesy with the Very Long Baseline Array, *Journal of Geodesy*, 83(9), 859-876
- Prawirodirdjo, L., and Bock, Y. (2004), Instantaneous global motion model from 12 years of continuous GPS observations, *Journal of Geophysical Research*, 109, B08405, doi: 10.1029/2003JB002944.
- Qian, B., and Rasheed, K. (2004), Hurst exponent and financial market predictability. In: *Proceedings of the 2<sup>nd</sup> IASTED International Conference on Financial engineering and applications*, Cambridge, MA, USA, 203-209.
- Qian, B., and Rasheed, K. (2007), Stock market prediction with multiple classifiers, *Applied Intelligence*, 26, 25-33.
- Redondo, S. T., Salinas, A., Portí, J., Morente, J. A., Fornieles, J., Méndez, A., Galindo-Zaldívar, J., Pedrera, A., Ruiz-Constán, A., and Anahnah, F. (2010), Study of Schumann resonances based on magnetotelluric records from the western Mediterranean and Antarctica. *Journal of Geophysical Research*, 115, D22114, doi:10.1029/2010JD014316.

- 1  
2  
3  
4  
5  
6  
7  
8  
9  
10  
11  
12  
13  
14  
15  
16  
17  
18  
19  
20  
21  
22  
23  
24  
25  
26  
27  
28  
29  
30  
31  
32  
33  
34  
35  
36  
37  
38  
39  
40  
41  
42  
43  
44  
45  
46  
47  
48  
49  
50  
51  
52  
53  
54  
55  
56  
57  
58  
59  
60  
61  
62  
63  
64  
65
- Reilinger R. E, McClusky, S.C., Oral, M. B., King, R. W., and Toksoz, M .N. (1997). Global positioning system measurements of present-day crustal movements in the Arabia-Africa-Eurasia plate collision zone, *Journal of Geophysical Research*, 102, 9983-9999.
- Reilinger, R., McClusky, S., Vernant, P., Lawrence, S., Ergintav, S., Cakmak, R., Ozener, H., Kadirov, F., Guliev, I., Stepanyan, R., Nadariya, M., Hahubia, G., Mahmoud, S., Sakr, K., ArRajehi, A., Paradisis, D., Al-Aydrus, A., Prilepin, M., Guseva, T., Evren, E., Dmitrotsa, A., Filikov, S. V., Gomez, F., Al-Ghazzi, R., and Karam, G., (2006), GPS constraints on continental deformation in the Africa-Arabia-Eurasia continental collision zone and implications for the dynamics of plate interactions, *Journal of Geophysical Research*, 111, doi:10.1029/2005JB004051.
- Royer, J. Y., Gorden, R. G., DeMets, C., and Vogt, P. R. (1997), New limits on the motion between India and Australia since chron 5 (11 Ma) and implications for lithospheric deformation in the equatorial Indian Ocean, *Geophysical Journal International*, 129, 41-74.
- Ryan, J. W., and Ma, C. (1989), NASA Crustal Dynamics Project results: Tectonic plate motions measured on a global scale with VLBI (abstract), *Eos Transactions*, 70, 304.
- Scherneck, H. G. (1991), A parameterized solid earth tide model and ocean tide loading effects for global geodetic baseline measurements. *Geophysical Journal International*, 106, 677-694.
- Schlüter, W., and Behrend, D. (2007), The International VLBI Service for Geodesy and Astrometry (IVS): current capabilities and future prospects, *Journal of Geodesy*, 81, 379-387.

- 1 Schuh, H., and Behrend, D. (2012), VLBI: A fascinating technique for geodesy and  
2 astrometry, *Journal of Geodynamics*, 61, 68-80.  
3  
4  
5 Schuh H., and J. Böhm, (2013), Very Long Baseline Interferometry for Geodesy and  
6 Astrometry, In Guochang Xu (editor): *Sciences of Geodesy II, Innovations and Future*  
7 *Developments*, Springer Verlag, doi: 10.1007/978-3-642-28000-9.  
8  
9  
10  
11  
12  
13 Sella, G. F., Dixon, T. H., and Mao, A. (2002), REVEL: A model for recent plate velocities  
14 from space geodesy, *Journal of Geophysical Research*, 107, doi:  
15 10.1029/2000JB000033.  
16  
17  
18  
19  
20  
21  
22 Sempere, J. C., and Klein, M. (1995), New Insights in the Crustal accretion from Indian  
23 Ocean spreading centers. *Eos Transactions*, 76 (11), 113-116.  
24  
25  
26  
27 Serpelloni, E., Vannucci, G., Pondrelli, S., Argnani, A., Casula, G., Anzidei, M., Baldi, P.,  
28 and Gasperini, (2007), Kinematics of the western Africa-Eurasia plate boundary from  
29 local mechanisms and GPS data, *Geophysical Journal International*, 169, 1180-1200.  
30  
31  
32  
33  
34  
35  
36 Shen, Z. K., Zhao, C., Yin, A., Li, Y., Jackson, D. D., Fang, P., and Dong, D. (2000).  
37 Contemporary crustal deformation in east Asia constrained by Global positioning  
38 system measurements, *Journal of Geophysical Research*, 105, 5721-5734.  
39  
40  
41  
42  
43  
44 Simons, W. J. F., Socquet, A., Vigny, C., Ambrosius, B. A. C., Abu, S. H., Promthong, C.,  
45 Subarya, C., Sarsito, D. A., Matheussen, S., Morgan, P., and Spakman, W. (2007), A  
46 decade of GPS in Southeast Asia: Resolving Sundaland motion and boundaries,  
47 *Journal of Geophysical Research*, 112, B06420, doi:10.1029/2005JB003868.  
48  
49  
50  
51  
52  
53  
54  
55 Small, C. (1995), Observations of ridge-hotspot interactions in the Southern Ocean. *Journal*  
56 *of Geophysical Research*, 100, 17931-17946.  
57  
58  
59  
60  
61  
62  
63  
64  
65

- 1  
2  
3  
4  
5  
6  
7  
8  
9  
10  
11  
12  
13  
14  
15  
16  
17  
18  
19  
20  
21  
22  
23  
24  
25  
26  
27  
28  
29  
30  
31  
32  
33  
34  
35  
36  
37  
38  
39  
40  
41  
42  
43  
44  
45  
46  
47  
48  
49  
50  
51  
52  
53  
54  
55  
56  
57  
58  
59  
60  
61  
62  
63  
64  
65
- Smith, D. E., Kolenkiewicz, R., Dunn, P. J., Robbins, J. W., Torrence, M. H., Klosko, S. M.,  
Williamson, R. G., Pavlis, E. C., and Douglas, N. B. (1990), Tectonic motion and  
deformation from Satellite Laser Ranging to LAGEOS, *Journal of Geophysical  
Research*, 95, 22013-22041.
- Teke, K., Böhm, J., Nilsson, T., Spicakova, H., and Schuh, H. (2010), Intra-Eurasia plate  
motions based on EUREF, IVS-Europe, and IVS-combined solutions, 15<sup>th</sup> General  
Assembly of WEGENER, Bogazici University, September 14-17, 2010, Istanbul.
- Tao, Z., Jian, L., and Yao, G. J. (2011), Interaction between hotspots and the Southwest  
Indian Ridge during the last 90 Ma: Implications on the formation of oceanic plateaus  
and intra-plate seamounts, *Science China Earth Sciences*, 54, 1177-1188.
- Tregoning, P. (2002), Plate kinematics in the western Pacific derived from geodetic  
observations, *Journal of Geophysical Research*, 107, 2020,  
doi:10.1029/2001JB000406.
- Vergnolle, M., Calais, E., and Dong, L. (2007), Dynamics of continental deformation in Asia,  
*Journal of Geophysical Research*, 112 ( B11403), doi:10.1029/2006JB004807.
- Ward, S. N. (1990), Pacific-North America Plate Motions: New Results From Very Long  
Baseline Interferometry, *Journal of Geophysical Research*, 95, 21965-21981.
- Whitney, A. R., Rogers, A. E. E., Hinteregger, H. F., Knight, C. A., Lippincott, S., Levine, J.  
I., Clark, T. A., Shapiro, I. I., and Robertson, D. S. (1976), A very-long-baseline  
interferometer system for geodetic applications, *Radio Science*, 11(5), 421-432
- Yadav, R. K., Kundu, B., Gahalaut, K., Catherine, J., Gahalaut, V., Ambikapathy, A., and  
Naidu, M. S. (2013), Coseismic offset due to the 11 April 2012 Indian Ocean

1 earthquakes (Mw 8.6 and 8.2) derived from GPS measurements, Geophysical Research  
2 Letters, 40, 3389-3393.  
3

4  
5 Yen I. L., Leone, P., Watson, G. A., Zao, J. K., Popelar, J., Petrachenko, W. T., Feil, G.,  
6 Cannon, W.H., Mathieu, P., Newby, P., Tan, H., Wietfeldt, R. D., and Galt, J. A.  
7  
8 (1991), The Canadian geophysical long baseline interferometer, Radio Science, 26 (1),  
9  
10 89-99.  
11  
12  
13  
14  
15  
16  
17  
18  
19  
20  
21  
22  
23  
24  
25  
26  
27  
28  
29  
30  
31  
32  
33  
34  
35  
36  
37  
38  
39  
40  
41  
42  
43  
44  
45  
46  
47  
48  
49  
50  
51  
52  
53  
54  
55  
56  
57  
58  
59  
60  
61  
62  
63  
64  
65

## Tables

**Table 1:** The five different VLBI stations used in this study and their details.

| VLBI station Name and Country/Plate                   | IVS code | Latitude (Deg) | Longitude (Deg) | Height (m) |
|---|----------|----------------|-----------------|------------|
| WETTZELL<br>Germany/<br>Eurasian plate                | Wz       | 49.1450 N      | 12.8772 E       | 661        |
| HARTRAO<br>South Africa/African<br>plate              | Hh       | 2.8898 S       | 27.6854 E       | 1415       |
| SYOWA<br>Antarctica/Antarctic<br>plate                | Sy       | 69.0063 S      | 39.5863 E       | 51         |
| HOBART<br>Australia/ Australian<br>plate              | Ho       | 42.8019 S      | 147.4387 E      | 41         |
| SESHAN<br>China/Eurasian plate<br>[south China block] | Sh       | 31.0992 N      | 121.1996 E      | 5          |



**Table 2:** Details of the VLBI sessions and data duration

| Between the stations | Data from | Data to  | Number of sessions used for analysis |
|----------------------|-----------|----------|--------------------------------------|
| Hh-Sy                | 1999.858  | 2008.375 | 39                                   |
| Ho-Sh                | 1989.965  | 2011.140 | 62                                   |
| Sy-Ho                | 1999.858  | 2010.984 | 44                                   |
| Wz-Hh                | 1987.026  | 2013.075 | 545                                  |
| Wz-Sh                | 1990.256  | 2012.962 | 151                                  |

**Table 3:** Average baseline length, annual baseline length rate and the strain rate calculated for the five VLBI experiment pairs

| Station pair            | Baseline length (m) | Baseline length rate/year | Strain rate                |
|-------------------------|---------------------|---------------------------|----------------------------|
| HartRAO-Syowa (Hh-Sy)   | 4741786.094         | +13.5 mm/yr               | +2.84 x 10 <sup>-9</sup>   |
| Syowa-Hobart (Sy-Ho)    | 6035892.681         | +59.0 mm/yr               | +9.77 x 10 <sup>-9</sup>   |
| Wetzell-HartRAO (Wz-Hh) | 7832322.470         | -3.9 mm/yr                | -4.97 x 10 <sup>-10</sup>  |
| Hobart-Seshan (Ho-Sh)   | 7965495.893         | -54.8 mm/yr               | -6.87 x 10 <sup>-9</sup>   |
| Wetzell-Seshan (Wz-Sh)  | 8003555.664         | +3.6 mm/yr                | + 4.49 x 10 <sup>-10</sup> |

**Table 4:** The computed spectral indices of the baseline length time series for the studied VLBI pairs and the Hurst exponents computed from the corresponding spectral index values.

| Baseline lengths<br>between the stations | Spectral index<br>( $V$ ) | Hurst exponent<br>( $H$ ) |
|--|---------------------------|---------------------------|
| HartRAO-Syowa (Hh-Sy)                    | 1.715±0.346               | 0.357                     |
| Syowa-Hobart (Sy-Ho)                     | 1.715±0.317               | 0.357                     |
| Wettzell-HartRAO (Wz-Hh)                 | 1.717±0.085               | 0.358                     |
| Hobart-Seshan (Ho-Sn)                    | 1.716±0.264               | 0.358                     |
| Wettzell-Seshan (Wz-Sn)                  | 1.716±0.164               | 0.358                     |

## Figure Captions

**Figure 1:** Major tectonic plates and their boundaries shown over the topographic relief map of the Eastern hemisphere. Some of the microplates, tectonic blocks, and tectonic features relevant to this study are also shown. Location of the five VLBI sites and the baseline lengths analyzed, along with their average values and annual rates are shown. SWIR-South West Indian Ridge; SEIR-South East Indian Ridge; CIR- Central Indian Ridge; RTJ- Rodrigues Triple Junction; OTJ- Owen Triple Junction.

**Figure 2:** Time series of baseline lengths (circles) estimated for the experiments made between VLBI sites (a) HartRAO-Syowa (b) Hobart-Seshan (c) Syowa-Hobart (d) Wettzell-HartRAO and (e) Wettzell-Seshan. The grey line represents the least-squares fitting for the baseline time series, the slope of which gives the rate of baseline change per year. The computed power spectra (blue line) and the spectral index value for the respective time series are also shown in the bottom panel.



Figure 1

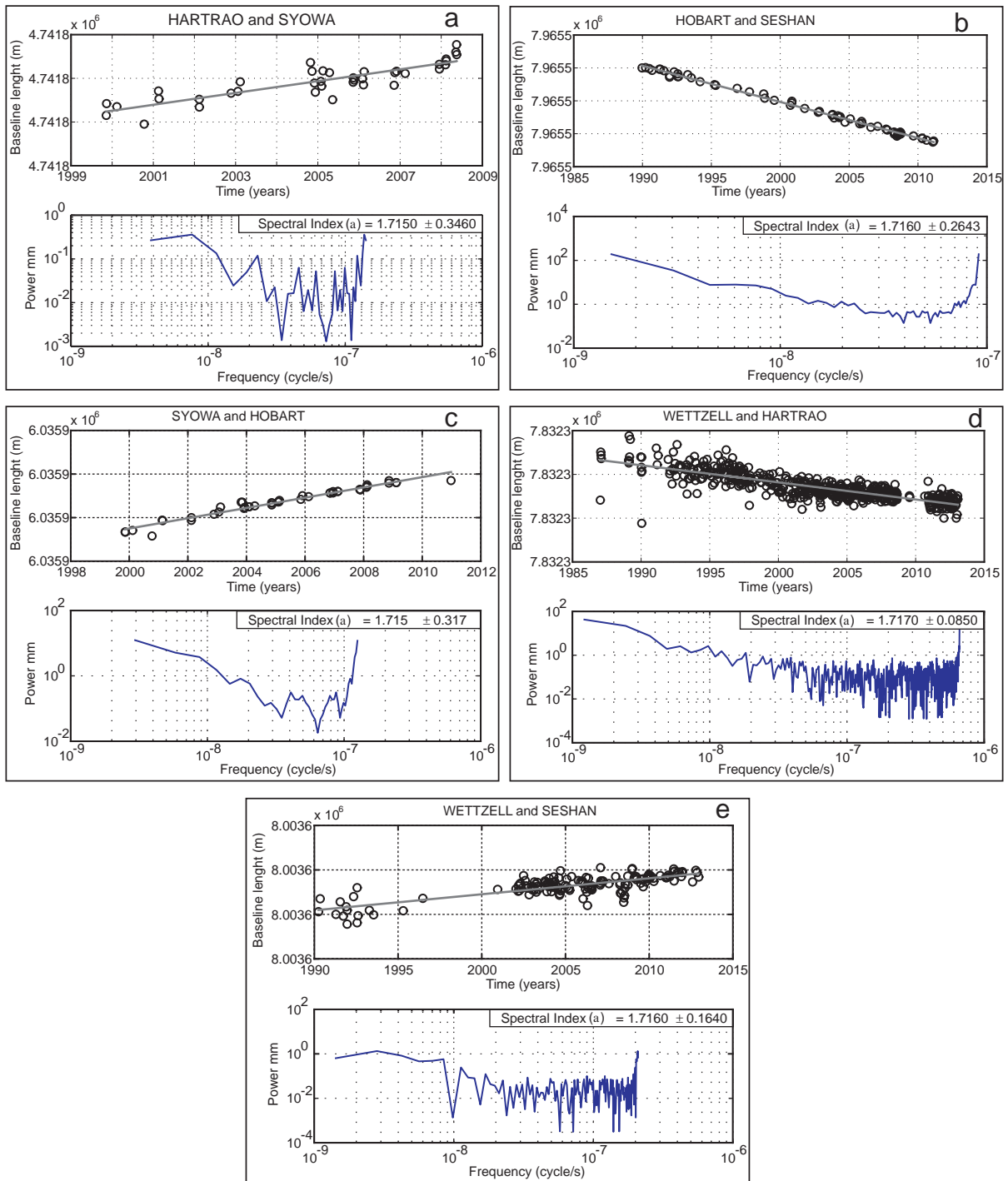


Figure 2